THE AMERICAN SOCIETY OF MECHANICAL ENGINEERS
345 E. 47th St., New York, N.Y. 10017

98-GT-105

MODE LOCALIZATION OF A CRACKED BLADE-DISKS

J. H. Kuang and B. W. Huang

Department of Mechanical Engineering
National Sun Yat-Sen University
Kaohsiung, TAIWAN, R. O. C.

(Phone:+886-7-525-2000 FAX:+886-7-5254299 E-Mail: kuang@mail.nsysu.edu.tw)

ABSTRACT

In this paper, the effect of blade crack on the mode localization of a rotating blade-disk is studied. Pretwisted taper beams are used to simulate blades of a blade-disk. The crack on the blade can be regarded as a local disorder of this periodically coupled blades system. An application of Hamilton's principle and Galerkin's method is used to formulate the equations of motion of the mistuned system. Effects of pretwisted angle, rotating speed and crack depth of the blade on the in-plane and off-plane mode localizations of a rotating system are investigated. Numerical results indicate that the increase of rotating speed, pretwisted angle and crack depth could enhance the localization phenomenon significantly.

Keywords: Mode Localization, Crack, Blade-Disk

NOMENCLATURE

A = cross section area of the each blade
a = depth of crack
b_0 = width at the root of the blade
b_l = width at the tip of the blade
E = Young's modulus of material of blade
$\{\overline{F}\}$ = external force vector
k_s = the stiffness of coupling for sth blade
L = length of blade
N = total number of blades
P_b = bending monent at crack
$p_i^s(t)$, $q_i^s(t)$ = determined coefficient for transverse direction for the sth blade, $i = 1, 2, \ldots, m$
r = arbitrary position on the blade
r_c = position of coupled spring
r^* = cracked position on the blade
R_h = inner diameter of disk
r = arbitrary position on the blade
s = the number of blade
t_0 = thickness at the root of the blade
t_l = thickness at the tip of the blade
$u_s(r,t)$, $v_s(r,t)$ = deflection in transverse direction of the sth blade for the rotational plane and out of plane
$u_\xi(r,t)$, $v_\xi(r,t)$ = deflection in transverse direction of the cracked blade for the rotational plane and out of plane
$\phi_i^s(r)$ = comparison functions for the sth blade
λ_i = coefficient
μ = Poisson' s Ratio
ξ = the number of cracked blade
θ = the pretwisted angle of blade
ρ = density of blade
Ω = rotation speed
ω = excitating frequency on the system
ω_0, ω_n = reference and natural frequency of the system

1. INTRODUCTION

The localization phenomenon may be observed in a weakly coupled periodic structure with local structural or material irregularities. Such localization may in turn localize the vibrational modes and thereby confine the vibrational energy. A number of studies were conducted to introduce the mode localization phenomenon in mistuned periodic structures [Bendiksen (1987), Pierre and Dowell (1987), Wei and Pierre (1988a, 1988b)]. However, Different models and parameter values used in the above analyses have yielded different and even conflicting conclusions.

Presented at the International Gas Turbine & Aeroengine Congress & Exhibition
Stockholm, Sweden — June 2–June 5, 1998
This paper has been accepted for publication in the Transactions of the ASME
Discussion of it will be accepted at ASME Headquarters until September 30, 1998

Due to manufacturing flaws or cyclic fatigue during operation, cracks frequently appear in the rotating machinery. Especially for the turbo-disk, numerous cracks were observed after severe operation [Bernstein and Allen (1992), Walls, deLaneuville and Cunningham (1997)]. The local structural irregularity caused by cracks on the blade may change the dynamic behavior of this mistuned system. The effect of crack on the dynamic and static behaviors of structures have been studied by a number of papers [Rizos, Aspragathos and Dimarogonas (1990), Broke (1986), Tada *et al.* (1973)]. More recent papers by Chen *et al.* (1988) and Grabowski (1980) also dealt with the effect of crack on a rotating machinery. The shrouded bladed disk of a turbo-rotor can be regarded as a periodic system if all the blades are assembled periodically. The dynamic behavior of such shrouded blade-disk system has been studied by Cottney and Ewins (1974), whereas the fundamental aspects of mode localization in mistuned turbomachinery rotors have been studied by Bendiksen (1984) and Kaneko et al (1994). More recent studies by Cha and Pierre (1991), and Orgun and Tongue (1994) have dealt with vibrational localization in the mistuned system with multi-mode subsystem.

Design of turbomachinery trend toward more and more high efficiency, so complex shape of blade in turbomachinery is unavoidable. To consider the shape effect of blade on the dynamic behaviors of a turbo-disk, periodically coupled taper beams are used herein to simulate blades of the turbo-disk. For the sake of simplicity, the tapered pretwisted beams are approximated as Euler-Bernoulli beams. Similar models were proposed by those of Rao (1977), and Young (1991). Most of these studies on mode localization are limited to stationary mistuned structures. The shrouded effect, commonly treated as a massless spring effect, is considered in this study in order to introduce the constraint between blades. The effects of crack size, pretwisted angle and rotation speed on the in-plane and off-plane mode localizations in the shrouded blade-disk have been investigated in this study.

2. EQUATIONS OF MOTION

The periodic shrouded blade structure at a constant rotating speed Ω is sbown in Fig. 1(a). It consists of a rigid hub with radius R_h and a cyclic assembly of N coupled blades. Each blade is coupled with the adjacent one through a shroud. The length of cantilever beam is L, and every blade is coupled by a shroud ring to the adjacent one at position r_c. The individual blade modeled as the tapered pretwisted beam is displayed in Fig. 1(b). The thickness and breadth at the root of the blade are t_0 and b_0. The deflection components $v_s(r,t)$ and $u_s(r,t)$ denote respectively the transverse flexible deflection of the sth blade in the rotational plane and perpendicular to the rotational plane.

2.1 Blades without crack

In this paper, it is assumed that the cross-section of the blade is symmetric about two principle axes and only the flexural bending

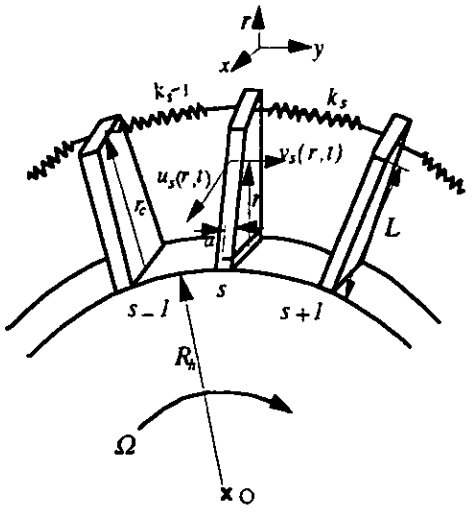

(a) Geometry of the blade-disk system

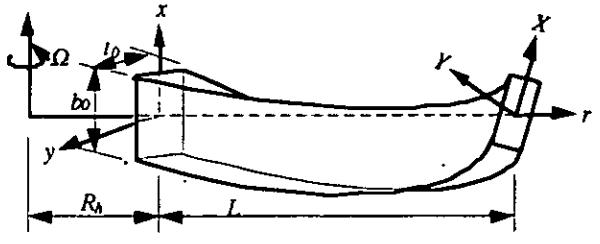

(b) Geometry of the pretwisted taper blade

Figure 1 Geometry of a rotating blade-disk

is able to occur. The kinetic energy, due to the bending vibration, of the rotating sth taper blade is given by

$$T_s = \frac{1}{2}\int_0^L \rho A \left\{ \left[\dot{u}_s(r,t)\right]^2 + \left[\dot{v}_s(r,t)\right]^2 + \left[\Omega v_s(r,t)\right]^2 \right\} dr \qquad (1)$$

The cross sectional area of the taper beam at position r is

$$A(r) = b_0 t_0 \left(1 - \alpha \frac{r}{L}\right)\left(1 - \beta \frac{r}{L}\right) \qquad (2)$$

and

$$\alpha = \frac{b_0 - b_1}{b_0} \qquad (3)$$

$$\beta = \frac{t_0 - t_1}{t_0} \qquad (4)$$

where b_1 and t_1 denote respectively the breadth and thickness at the blade tip.

The total strain energy of the sth blade consists of three terms, and each will be considered separately. The first is due to the bending moment and is

$$U_s^e = \frac{1}{2}\int_0^L E\left[I_{yy}(u_s'')^2 + 2I_{xy}(u_s'')(v_s'') + I_{xx}(v_s'')^2\right]dr \quad (5)$$

where a symbol prime (') denotes a partial derivative with respect to r. In this equation, E is the Young's modulus of the blade and I_{xx}, I_{yy} and I_{xy} are the moments of area. Consider the taper beam to be pretwisted with a uniform twist angle θ, and then the moments of area at the position r can be derived as

$$I_{xx} = I_{XX}\cos^2\left(\frac{r}{L}\theta\right) + I_{YY}\sin^2\left(\frac{r}{L}\theta\right) \quad (6a)$$

$$I_{yy} = I_{XX}\sin^2\left(\frac{r}{L}\theta\right) + I_{YY}\cos^2\left(\frac{r}{L}\theta\right) \quad (6b)$$

$$I_{xy} = (I_{YY} - I_{XX})\sin\left(\frac{r}{L}\theta\right)\cos\left(\frac{r}{L}\theta\right) \quad (6c)$$

where

$$I_{XX} = \frac{b_0 t_0^3}{12}\left(1-\alpha\frac{r}{L}\right)\left(1-\beta\frac{r}{L}\right)^3 \quad (7a)$$

$$I_{YY} = \frac{b_0^3 t_0}{12}\left(1-\alpha\frac{r}{L}\right)^3\left(1-\beta\frac{r}{L}\right) \quad (7b)$$

The strain energy component due to the centrifugal force caused by the rotational speed Ω can be derived as

$$U_s^\Omega = \frac{1}{2}\int_r^L p^*\left[(u_s')^2 + (v_s')^2\right]dr \quad (8)$$

where p^* is the centrifugal force, and is written by

$$p^* = \int_r^L \rho A\Omega^2(r + R_h)\,dr \quad (9)$$

The third and last term is the strain energy due to the elastic deformation of the shroud constrainer. This part is

$$U_s^k = \frac{k_s}{2}\left[v_{s+1}(r_c) - v_s(r_c)\right]^2 \quad (10)$$

Combining the three terms, the total strain energy of the sth blade can be obtained as follows.

$$U_s = U_s^e + U_s^\Omega + U_s^k \quad (11)$$

By means of Hamilton's principle, the equation of motion of the sth blade can be derived as

$$\rho A\ddot{u}_s - \rho\Omega^2\left[\int_r^L A(r+R_h)dr\,u_s'\right]' + E\left(I_{yy}u_s'' + I_{xy}v_s''\right)'' = 0 \quad (12a)$$

$$\rho A\ddot{v}_s - \rho\Omega^2\left\{Av_s + \left[\int_r^L A(r+R_h)\,dr\,v_s'\right]'\right\} + E\left(I_{xx}v_s'' + I_{xy}u_s''\right)'' = 0 \quad (12b)$$

and the boundary conditions are

$$u_s = v_s = u_s' = v_s' = 0, \quad \text{at} \quad r = 0 \quad (13a)$$

$$u_s'' = v_s'' = u_s''' = v_s''' = 0, \quad \text{at} \quad r = L \quad (13b)$$

The coupled blades are constrained with each other at tips $r=r_c$. The constraint of the sth blade is

$$k_s\left[v_s(r_c,t) - v_{s+1}(r_c,t)\right] + k_{s-1}\left[v_s(r_c,t) - v_{s-1}(r_c,t)\right] = 0 \quad (14)$$

Solutions of the above eigenvalue problem, i.e., Eqs (12a) and (12b), are assumed in the form

$$u_s(r,t) = \sum_{i=1}^m p_i^s(t)\,\phi_i^s(r) \quad (15a)$$

$$v_s(r,t) = \sum_{i=1}^m q_i^s(t)\,\phi_i^s(r) \quad (15b)$$

where $p_i^s(t)$ and $q_i^s(t)$ are coefficients to be determined and $\phi_i^s(r)$ are comparison functions. In order to simplify the notations, two dimensionless variables $\bar{r} = r/L$ and $\bar{r}_c = r_c/L$ are introduced. The deflection modes are used to approximate the comparison functions $\phi_i^s(\bar{r})$ in this article. They are

$$\phi_i^s(\bar{r}) = (\cosh\lambda_i\bar{r} - \cos\lambda_i\bar{r}) - \frac{\cos\lambda_i + \cosh\lambda_i}{\sin\lambda_i + \sinh\lambda_i}(\sinh\lambda_i\bar{r} - \sin\lambda_i\bar{r}) \quad (16)$$

and $\cos\lambda_i\bar{r}\cosh\lambda_i\bar{r} + 1 = 0$ for $i = 1, 2, \cdots, m$ (17)

By using the Galerkin's method, the equation of motion of the sth blade can be derived in matrix form as

$$[m]_s\begin{Bmatrix}\ddot{p}\\ \ddot{q}\end{Bmatrix}_s + \left([k^e]_s + [k^\Omega]_s\right)\begin{Bmatrix}p\\ q\end{Bmatrix}_s - k_{s-1}\left[\Lambda^{s-1}\right]\begin{Bmatrix}p\\ q\end{Bmatrix}_{s-1}$$
$$+(k_s + k_{s-1})\left[\Lambda^s\right]\begin{Bmatrix}p\\ q\end{Bmatrix}_s - k_s\left[\Lambda^{s+1}\right]\begin{Bmatrix}p\\ q\end{Bmatrix}_{s+1} = 0$$

for $s = 1, 2, \ldots, N$ (18)

where matrices $[m]_s$, $[k^e]_s$ and $[k^\Omega]_s$ are given as

$$[m]_s = \begin{bmatrix}[m]^u & 0\\ 0 & [m]^v\end{bmatrix}_s \quad (19a)$$

$$[k^e]_s = \begin{bmatrix}[k^e]^u & [k^e]^{uv}\\ [k^e]^{uv} & [k^e]^v\end{bmatrix}_s \quad (19b)$$

$$[k^\Omega]_s = \begin{bmatrix}[k^\Omega]^u & 0\\ 0 & [k^\Omega]^v\end{bmatrix}_s \quad (19c)$$

with

$$(m)_{ij}^u = (m)_{ij}^v = \int_0^1 A(\bar{r})\phi_i(\bar{r})\phi_j(\bar{r})d\bar{r} \quad (20a)$$

$$(k^e)_{ij}^u = \frac{E}{L^4}\int_0^1 I_{yy}(\bar{r})\phi_i''(\bar{r})\phi_j''(\bar{r})d\bar{r} \quad (20b)$$

$$(k^e)^v_{ij} = \frac{E}{L^4}\int_0^1 I_{xx}(\bar{r})\phi_i''(\bar{r})\,\phi_j''(\bar{r})\,d\bar{r} \tag{20c}$$

$$(k^e)^{uv}_{ij} = \frac{E}{L^4}\int_0^1 I_{xy}(\bar{r})\phi_i''(\bar{r})\,\phi_j''(\bar{r})\,d\bar{r} \tag{20d}$$

$$(k^\Omega)^u_{ij} = \frac{\rho\Omega^2}{L^2}\int_0^1 p^*(\bar{r})\phi_i'(\bar{r})\phi_j'(\bar{r})\,d\bar{r} \tag{20e}$$

$$(k^\Omega)^v_{ij} = \frac{\rho\Omega^2}{L^2}\int_0^1 \left[p^*(\bar{r})\phi_i'(\bar{r})\phi_j'(\bar{r}) - L^2 A(\bar{r})\phi_i(\bar{r})\phi_j(\bar{r})\right]\bar{d}r \tag{20f}$$

For the sake of convenience, the same comparison function is assumed for the individual blade of disk, i.e., $\phi_j^s(\bar{r}) \equiv \phi_j(\bar{r})$. So, matrices $\left[\Lambda^{s-1}\right]$, $\left[\Lambda^s\right]$ and $\left[\Lambda^{s+1}\right]$ are identical, and the vector $\{\phi(\bar{r})\}_s = \left[\phi_1^s(\bar{r}),\ \phi_2^s(\bar{r}),\cdots\phi_m^s(\bar{r})\right]^T$ defined. They can be rewritten as

$$\left[\Lambda^{s-1}\right] = \left[\Lambda^s\right] = \left[\Lambda^{s+1}\right] = \left[\Lambda\right] \tag{21}$$

$$[\Lambda] = \begin{bmatrix} 0 & 0 \\ 0 & \{\phi\}_s\{\phi\}_s^T \end{bmatrix}\Bigg|_{\bar{r}=\bar{r}_c} \tag{22}$$

2.2 Blade with a crack

Considering a crack be located at $\bar{r} = \bar{r}^*$ of the ξth blade, it may be regarded as a mistuned system. The total strain energy of the defective blade will consist of four terms.

$$U_\xi = U_\xi^e + U_\xi^\Omega + U_\xi^k - U_\xi^c \tag{23}$$

where U_ξ^c is the released energy of the crack for the ξ blade. If the crack is initiated by the bending fatigue, the mode I loading will dominate the stress field. According to Dimarogonas's (1983) and Krawczuk's (1993) investigations, alteration of elastic deformation energy in places of the crack caused by bending moment is the only important change in the case of slender beams. Therefore, the released energy of this crack may be written in the form:

$$U_\xi^c = b_0(1-\alpha\bar{r}^*)\int_0^a \frac{(1-\mu^2)}{E}K_I^2\,da \tag{24}$$

where a, μ are the depth of crack and the Poisson's ratio of blade, and K_I is the stress intensity factor under mode I loading. In this case the mode I stress intensity factor K_I can be approximated by Tada *et al.* (1973) equation as

$$K_I = \frac{6p_b}{t_0^2 b_0(1-\alpha\bar{r}^*)(1-\beta\bar{r}^*)^2}\sqrt{\pi\bar{\gamma}t_0(1-\beta\bar{r}^*)}\,F_I(\bar{\gamma}) \tag{25}$$

where the variables for a near root crack can be approximated by

$$p_b = EI_{xx}v_\xi''\Big|_{\bar{r}=\bar{r}^*} \tag{26}$$

$$\bar{\gamma} = \frac{a}{t_0(1-\beta\bar{r}^*)} \tag{27}$$

$$F_I(\bar{\gamma}) = \sqrt{\frac{2}{\pi\bar{\gamma}}\tan\left(\frac{\pi\bar{\gamma}}{2}\right)}\,\frac{0.923+0.199\left[1-\sin\left(\frac{\pi\bar{\gamma}}{2}\right)\right]^4}{\cos\left(\frac{\pi\bar{\gamma}}{2}\right)} \tag{28}$$

Adapting Eq. (24) gives

$$U_\xi^c = 3E\left(1-\mu^2\right)t_0(1-\beta\bar{r}^*)\int_0^1 I_{xx}Q(\bar{\gamma})\left(v_\xi''\right)^2\delta(\bar{r}-\bar{r}^*)\,d\bar{r} \tag{29}$$

where $\delta(\bar{r}-\bar{r}^*)$ is the delta function and

$$Q(\bar{\gamma}) = \int_0^{\bar{\gamma}} \pi\,\bar{\gamma}\,F_I^2(\bar{\gamma})\,d\bar{\gamma} \tag{30}$$

Similarly, equations of motion for the ξth cracked blade can be derived by using Hamilton's principle. It leads to

$$\rho A\ddot{u}_\xi - p\Omega^2\left[\int_r^L A(r+R_h)dr\ u_\xi'\right]' + E\left(I_{yy}u_\xi'' + I_{xy}v_\xi''\right)'' = 0 \tag{31a}$$

$$\rho A\ddot{v}_\xi - \rho\Omega^2\left\{Av_\xi + \left[\int_r^L A(r+R_h)\,dr\ v_\xi'\right]'\right\} - 6EI_{xx}\left(1-\mu^2\right)t_0(1-\beta\bar{r}^*)Q(\bar{\gamma})\left[v_\xi''\delta(\bar{r}-\bar{r}^*)\right]'' + E\left(I_{xx}v_\xi'' + I_{xy}u_\xi''\right)'' = 0 \tag{31b}$$

Boundary conditions and constraint condition of Eqs (31a) and (31b) are the same as the sth blade, i.e., the blade without crack. Based on the Galerkin method, the equation of motion of the ξth cracked blade can be rewritten in matrix form as follows,

$$[m]_\xi\begin{Bmatrix}\ddot{p}\\ \ddot{q}\end{Bmatrix}_\xi + \left(\left[k^e\right]_\xi + \left[k^\Omega\right]_\xi - \left[k^c\right]_\xi\right)\begin{Bmatrix}p\\ q\end{Bmatrix}_\xi - k_{\xi-1}\left[\Lambda^{\xi-1}\right]\begin{Bmatrix}p\\ q\end{Bmatrix}_{\xi-1} + \left(k_\xi + k_{\xi-1}\right)\left[\Lambda^\xi\right]\begin{Bmatrix}p\\ q\end{Bmatrix}_\xi - k_\xi\left[\Lambda^{\xi+1}\right]\begin{Bmatrix}p\\ q\end{Bmatrix}_{\xi+1} = 0 \tag{32}$$

where

$$\left[k^c\right]_s = \begin{bmatrix} 0 & 0 \\ 0 & \left[k^{cv}\right] \end{bmatrix}_s \tag{33}$$

and

$$k_{ij}^{cv} = 6\frac{EI_{xx}}{L^4}\left(1-\mu^2\right)t_0(1-\beta\bar{r}^*)Q(\bar{\gamma})\left[\phi_i''(\bar{r})\phi_j''(\bar{r})\right]_{\bar{r}=\bar{r}^*} \tag{34}$$

2.3 Equation of motion of the mistuned system

For simplicity, the same comparison function is assumed for each blade. The equation of motion of the entire disk system can be expressed as

$$[M]\{\ddot{X}\}+[K]\{X\}=0 \tag{35}$$

The system mass matrix $[M]$ and the system stiffness matrix $[K]$ are

$$[M]=\begin{bmatrix} [m]_1 & 0 & 0 & . & 0 & 0 & 0 \\ 0 & [m]_2 & 0 & . & 0 & 0 & 0 \\ 0 & 0 & [m]_3 & . & 0 & 0 & 0 \\ . & . & . & . & . & . & . \\ 0 & 0 & 0 & . & [m]_{N-2} & 0 & 0 \\ 0 & 0 & 0 & . & 0 & [m]_{N-1} & 0 \\ 0 & 0 & 0 & . & 0 & 0 & [m]_N \end{bmatrix} \tag{36a}$$

$$[K]=\begin{bmatrix} [\alpha]_1 & -k_1[\Lambda] & 0 & . & 0 & 0 & -k_N[\Lambda] \\ -k_1[\Lambda] & [\alpha]_2 & -k_2[\Lambda] & . & 0 & 0 & 0 \\ 0 & -k_2[\Lambda] & [\alpha]_3 & . & 0 & 0 & 0 \\ . & . & . & . & . & . & . \\ 0 & 0 & 0 & . & [\alpha]_{N-2} & -k_{N-2}[\Lambda] & 0 \\ 0 & 0 & 0 & . & -k_{N-2}[\Lambda] & [\alpha]_{N-1} & -k_{N-1}[\Lambda] \\ -k_N[\Lambda] & 0 & 0 & . & 0 & -k_{N-1}[\Lambda] & [\alpha]_N \end{bmatrix} \tag{36b}$$

$$\{X\}=\left[\begin{Bmatrix} p \\ q \end{Bmatrix}_1^T, \begin{Bmatrix} p \\ q \end{Bmatrix}_2^T, \ldots, \begin{Bmatrix} p \\ q \end{Bmatrix}_{N-1}^T, \begin{Bmatrix} p \\ q \end{Bmatrix}_N^T\right]^T \tag{36c}$$

$$\{X\}=\{\bar{X}\}e^{i\omega t} \tag{36d}$$

Due to the cyclic arrangement of blades, it leads to $\begin{Bmatrix} p \\ q \end{Bmatrix}_{N+1}=\begin{Bmatrix} p \\ q \end{Bmatrix}_1$

and

$$[\alpha]_s=\left[k^e\right]_s+\left[k^\Omega\right]_s-\left[k^c\right]_s+k_s[\Lambda]+k_{s-1}[\Lambda] \tag{37}$$

$$k_0=k_N \tag{38}$$

3. NUMERICAL RESULTS AND DISCUSSIONS

A rigid hub attached to 46 uniform blades, which are modeled as tapered pretwisted beams, is used to approximate the bladed disk. In this article, the existence of mode localization for a mistuned, tapered pretwisted blade-disk system with a cracked blade is studied. The effects of rotational speed, depth of the crack, and pretwisted angle of the blade on the mode localization have also been studied. The following non dimensional parameters $(R_h/L)=0.2$, $(b_o/L)=0.1$, $(t_0/L)=0.02$, $\alpha=\beta=0.25$, $\theta=45^o$ and $\bar{r}^*=0$ are specified for the blade. For the convenience of specifying the mode localization frequency, a non-dimensional frequency ratio ω_n/ω_0 is employed. The frequency ω_n is the natural frequency of the mistuned system, and ω_0 is a reference frequency that is defined as $\omega_0=0.01\sqrt{\frac{E}{\rho L^2}}$.

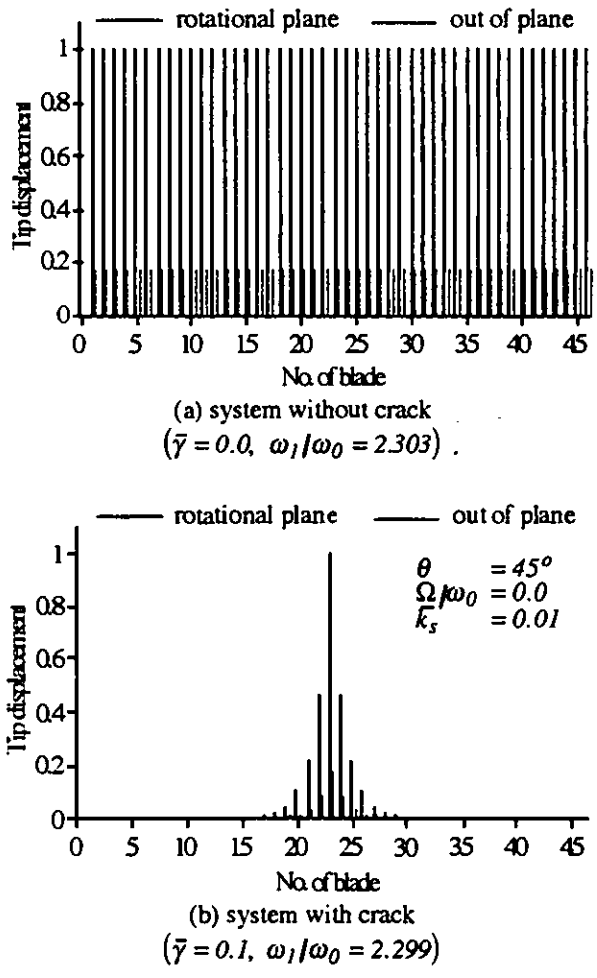

Figure 2 Tip displacement pattrens of the mistuned system with different crack depth (for the 1st mode)

As a crack propagates on a blade, it may not only alter the dynamic behavior of this blade, but may also introduce the so called mode localization phenomenon in the whole mistuned system. In this numerical example, a crack is assumed at the root of the 23rd blade.

3.1 Free vibration analysis

An assembly of 46 pretwisted taper beams interconnected at blade tip is considered, i.e., $\bar{r}_c=1$. An interblade coupling stiffness $\bar{k}_s=0.01$ is assumed for the shroud ring. The dimensionless stiffness is defined as $\bar{k}_s=\left(12k_sL^3\right)/Eb_0t_0^3$. The vibration of this pretwisted blade-disk system consists

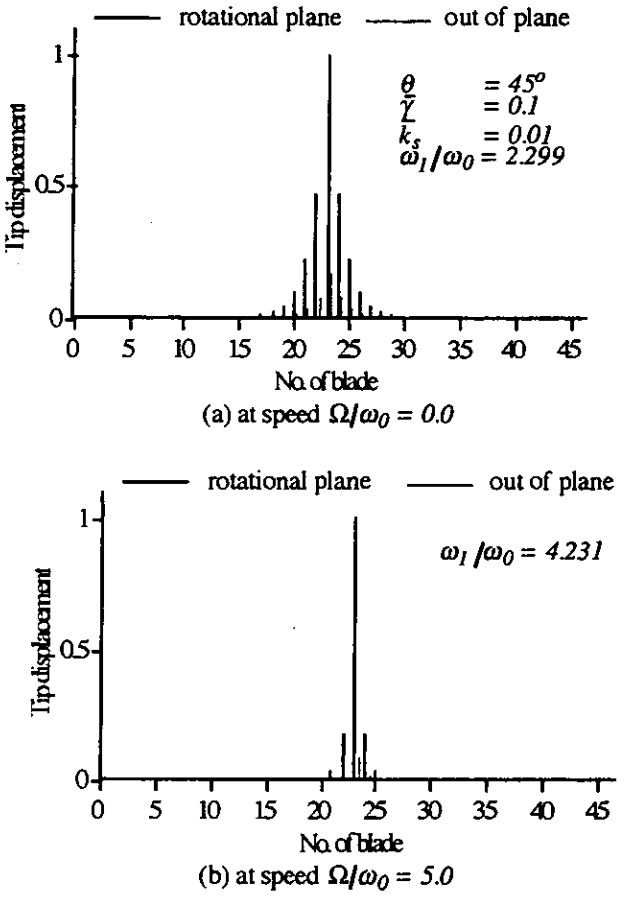

Figure 3 Tip displacement patterns of the mistuned system under different rotating speeds (for the 1st mode)

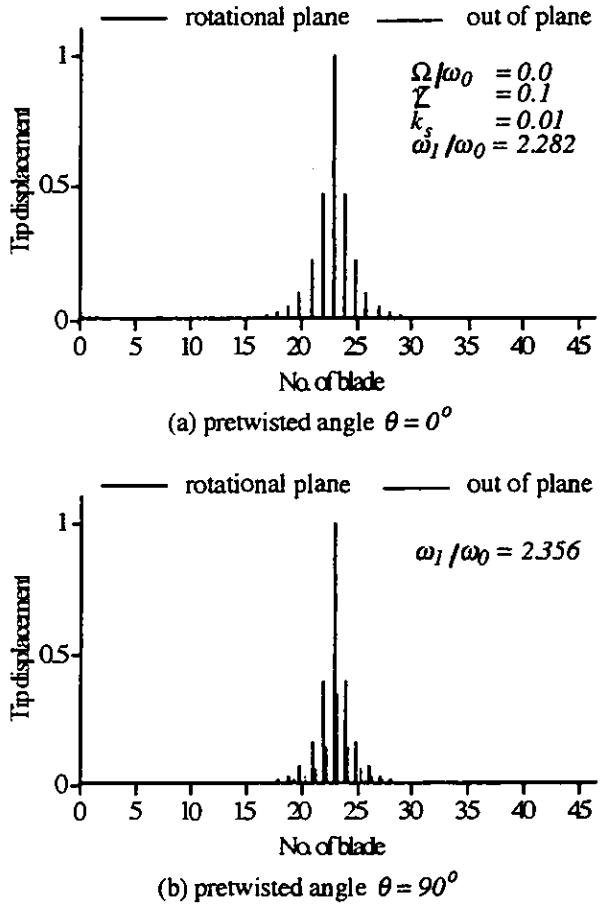

Figure 4 Tip displacements of the mistuned system for different pretwisted angles (for the 1st mode)

of two parts, one of which is vibrated in the rotational plane and the other is in the out-of-plane. Blade tip displacement patterns of the tuned system at the lowest natural frequency are illustrated in Fig. 2(a). The figure shows that the magnitude of tip displacement of the individual blade in a tuned system is the same. Figures 2(b) is illustration of the occurrence of modal localization in this mistuned system. Results indicate that the tip displacement pattern may change from a weak localization to a strong localization as the crack depth γ is increased. Figures 3(a) and (b) display that the mode localization is affected by the rotational speed. As expected, because of the centrifugal force, the localization frequency ω_l of the mistuned system is increased. It is also observed that the localization vibration in the rotational plane is enhanced and the vibration in the out of plane is depressed simultaneously as the rotational speed is increased. The effect of pretwisted angle on the mode localization has also been studied in this investigation. Figures 4(a) and (b) display the variation of the tip displacement pattern for blades with different pretwisted angle. It indicates that the localization in the out of plane is enhanced as the pretwisted angle is increased.

As noted in a number of papers, the degree of localization depends significantly upon the magnitude of disorder and the modal coupling effect. The modal coupling effect in this blade-disk system is determined by the spring stiffness constant $\bar{k}_s$, the blade mode number, and the modal deflection at the blade tip. The above study has shown that strong localization occurs in all modes for a small coupling stiffness, e.g., $\bar{k}_s = 0.01$ in this case. It is of interest to investigate what happens in the large coupling case. Figures 5(a) and (b) display selected mistuned systems connected at their tips for $\bar{k}_s = 1.0$. As the coupling stiffness is increased up to $\bar{k}_s = 1.0$, localization may turn out to be weak at the first order frequency ω_l as shown in Fig. 5(a). However, strong localization may reappear in the groups of modes whose primary component mode has a node near the constraint location $\bar{r}_c = 1$. Figure 5(b) shows the localization at the second order frequency and it shows a strong localization occurs in this mode.

3.2 Forced response

The response of the mistuned blade-disk system depends upon the disk structure, the excitation frequency and magnitude, the crack depth and the interblade coupling. The effects of blade twist angle, crack depth and rotating speed on the localization response have been studied. Consider a uniformly distributed harmonic force $\{\bar{F}\}e^{i\omega t}$ being applied on the tapered pretwisted blades of the mistuned system. The maximum amplitude responses of the tuned and mistuned systems are shown in Figs 6. Only a single peak at $(\omega_1/\omega_0) = 2.303$ is observed for the tuned system. It indicates that every individual blade possesses identical frequency at this peak. Contrary to the single peak in the tuned system, multiple peaks are found for the cracked blade. A group of peak amplitudes are appeared for this mistuned system in a wider frequency range. The lowest resonance frequency of this mistuned system, i.e., the so called localization frequency $(\omega_1/\omega_0) = 2.299$, is close but lower than the corresponding lowest natural frequency of a tuned system. From the tip pattern as shown in Fig. 2(b), it shows that the vibration at localization frequency is confined only in a few numbers of blades.

Figure 7 displays the displacement frequency responses of the mistuned system with different pretwisted angles. Results indicate that the higher localization frequency is observed for the mistuned system with large pretwisted angle. Figure 5 shows the corresponding tip displacement patterns. It show that the localization in the out of plane has been enhanced for the mistuned system with a larger pretwisted angle.

4. CONCLUSIONS

The effect of crack depth, twist angle and rotational speed on mode localization in a pretwisted blade-disk system has been investigated. The following conclusions can be drawn from this study.

(1) It can be observed that the localization phenomenon of a pretwisted shrouded blade-disk system may be introduced by a cracked blade. The strong localization appears for the mistuned system with weak interblade coupling. This localization may disappear as the interblade coupling is increased, but it will reappear in the higher modes.

(2) The depth of a crack is one of the important parameters for the modal localization of a rotating blade-disk system. Results indicate that the localization may be enhanced as the depth of the crack is increased.

(3) The rotational speed of the mistuned disk has a significant influence on the localization frequency; it will shift the localization frequency towards a higher frequency. The centrifugal force introduced by the rotational speed may enhance the localization in the rotational plane and depress it in the out of plane.

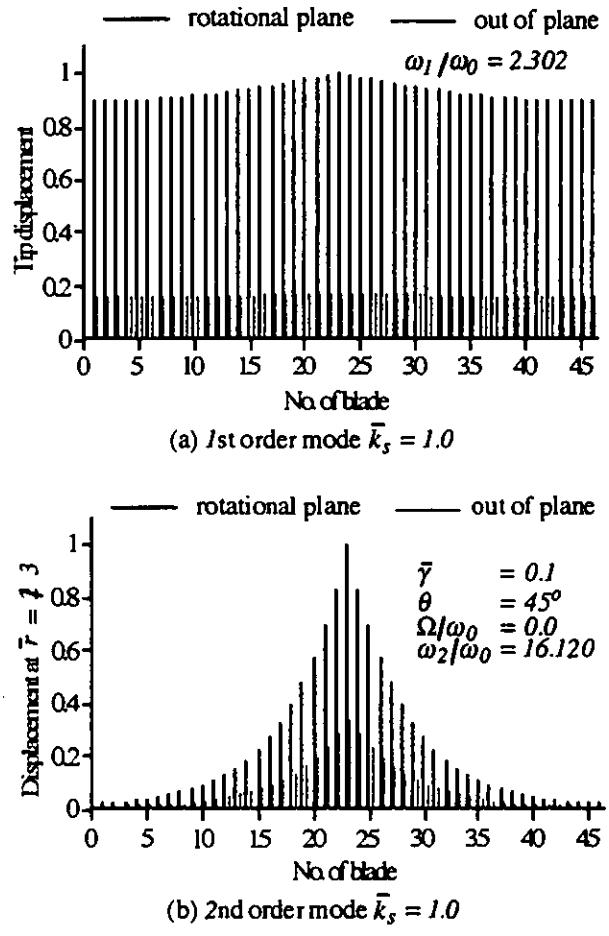

Figure 5 Displacement patterns of the mistuned system with strong modal coupling for the 1st and 2nd order modes

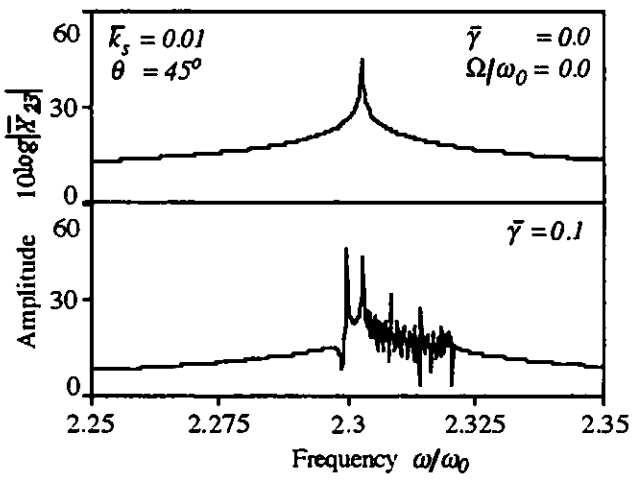

Figure 6 Varation of frequency response of systems with and without a crack

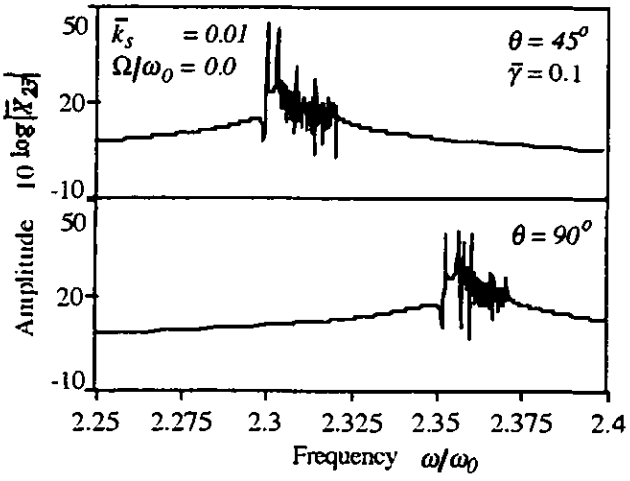

Figure 7 Varation of frequency response of systems with and without considering the rotational speed effect

(4) The twist angle of the blade may also affect localization in the mistuned pretwisted blade-disk system. A large twist angle will enhance modal localization in the out of plane.

5. REFERNCE

Bendiksen, O. O., 1984, "Flutter of Mistuned Turbo machinery Rotors," ASME *Journal of Engineering for Gas Turbines and Power*, Vol. 106, pp. 25-23

Bendiksen, O. O., 1987, "Mode Localization phenomena in Large Space Structures," AIAA *Journal*, Vol. 25, pp. 1241-1248.

Bernstein, H. L. and Alien, J. M., 1992, "Analysis of Cracked Gas Turbine Blades," ASME *Journal of Engineering for Gas Turbines and Power*, Vol. 114, pp. 293-301.

Broek D., 1986, *Elementary Engineering Fracture mechanics*, Martinus Nijhoff Publishers.

Cha, P. D. and Pierre, C., 1991, "Vibration Localization by Disorder in Assemblies of Monocoupled, Multimode Component Systems," ASME *Journal of Applied Mechanics*, Vol. 58 , pp. 1072-1081.

Chen L. and Chen C., 1988, "Vibration and Stability of Cracked Thick Rotating Blade," *Computers & Structures*, Vol. 28, No. 1, pp. 67-74.

Cottney, D. J. and Ewins, D. J., 1974, "Towards the Efficient Vibration Analysis of Shrouded Bladed Disk Assemblies," ASME *Journal of Engineering for Industry*, Vol. 96B, pp. 1054-1059.

Dimarogonas, A. D., and Paipetis, S. A., 1983, "*Analytical Methods in Rotor Dynamics*," Applied Science Publishers, New York.

Grabowski B., 1980, "The Vibrational Behavior of a Turbine Rotor Containing a Transverse Crack," ASME *Journal of Mechanic Design*, Vol. 102, pp. 140-146.

Kaneko, Y., Mase, M., Fujita, K., and Nagashima, T., 1994, "Vibration Response Analysis of Mistuned Bladed Disk," JSME *International Journal Series C*, Vol. 37, No. 1, pp. 33-40.

Krawczuk, M. and Ostachowicz, W. M., 1993, "Transverse Natural Vibrations of a Cracked Beam Loaded with a Constant Axial Force," ASME *Journal of Vibration and Acoustics*, Vol. 115, pp. 524-528.

Orgun C. O. and Tongue, B. H, 1994, "Mode Localization in Coupled Circular Plates," ASME *Journal of Vibration and Acoustics*, Vol. 116, pp. 286-294

Pierre, C. and Dowell, E. H., 1987, "Localization of Vibrations by Structural Irregularity," *Journal of Sound and Vibration*, Vol. 114, No. 3, pp. 549-564

Rao, J. S., 1977, "Vibration of Rotating, Pretwisted and Tapered Blades," *Mechanism and Machine Theory*, Vol. 12, pp. 331-337.

Rizos, P. F., Aspragathos, N. and Dimarogonas, A. D., 1990, "Identification of Crack Location and Magnitude in a Cantilever Beam from the Vibration Mode," *Journal of Sound and Vibration*, Vol. 138, pp. 381-388.

Tada H., Paris P. and Irwin G., 1973, *The Stress Analysis of Crack Handbook*, Hellertown, Pennsylvania : Del Research Corporation.

Walls, D. P., deLaneuville, R. E. and Cunningham, S. E., 1997, "Damage Tolerance Based Life Prediction in Gas Turbine Engine Blades under Vibratory High Cycle Fatigue," ASME *Journal of Engineering for Gas Turbines and Power*, Vol. 119, pp. 143-146.

Wei, S. T. and Pierre, C., 1988, "Localization Phenomena in Mistuned Assemblies with Cyclic Symmetry part I: Free Vibrations," ASME *Journal of Vibration, Acoustics, Stress, and Reliability in Design*, Vol. 110, pp. 429-438.

Wei, S. T. and Pierre, C., 1988, "Localization Phenomena in Mistuned Assemblies with Cyclic Symmetry part II :Forced Vibrations," ASME *Journal of Vibration, Acoustics, Stress, and Reliability in Design*, Vol. 110, pp. 439-449.

Young, T. H., 1991, "Dynamic Response of A Pretwisted, Tapered Beam with Non-constant Rotating Speed," *Journal of Sound and Vibration*, Vol. 150, No. 3, pp. 435-446.

Acknowledgments- The authors would like to acknowledge the support of the National Science Council, R. O. C., through grant no. NSC87-2212-E-110-004.